

# Fiber Optic Force Sensors for MRI-Guided Interventions and Rehabilitation: A Review

Hao Su\*, *Member, IEEE*, Iulian I. Iordachita, *Senior Member, IEEE*,

Junichi Tokuda, *Member, IEEE*, Nobuhiko Hata, *Member, IEEE*, Xuan Liu, *Member, IEEE*,  
Reza Seifabadi, *Member, IEEE*, Sheng Xu, Bradford Wood, Gregory S. Fischer, *Member, IEEE*

**Abstract**—Magnetic Resonance Imaging (MRI) provides both anatomical imaging with excellent soft tissue contrast and functional MRI imaging (fMRI) of physiological parameters. The last two decades have witnessed the manifestation of increased interest in MRI-guided minimally invasive intervention procedures and fMRI for rehabilitation and neuroscience research. Accompanying the aspiration to utilize MRI to provide imaging feedback during interventions and brain activity for neuroscience study, there is an accumulated effort to utilize force sensors compatible with the MRI environment to meet the growing demand of these procedures, with the goal of enhanced interventional safety and accuracy, improved efficacy and rehabilitation outcome. This paper summarizes the fundamental principles, the state of the art development and challenges of fiber optic force sensors for MRI-guided interventions and rehabilitation. It provides an overview of MRI-compatible fiber optic force sensors based on different sensing principles, including light intensity modulation, wavelength modulation, and phase modulation. Extensive design prototypes are reviewed to illustrate the detailed implementation of these principles. Advantages and disadvantages of the sensor designs are compared and analyzed. A perspective on the future development of fiber optic sensors is also presented which may have additional broad clinical applications. Future surgical interventions or rehabilitation will rely on intelligent force sensors to provide situational awareness to augment or complement human perception in these procedures.

**Index Terms**—Fiber optic sensor, Fabry-Perot interferometer (FPI), fiber Bragg grating (FBG), haptics, image-guided interventions, percutaneous interventions, rehabilitation, neuroscience, MRI compatible robot.

H. Su is with the Wyss Institute for Biologically Inspired Engineering and the John A. Paulson School of Engineering and Applied Sciences, Harvard University, Cambridge, MA 02138, USA. (e-mail: haosu.ieee@gmail.com)

I. I. Iordachita is with the Johns Hopkins University, Baltimore MD, 21218, USA (e-mail: iordachita@jhu.edu)

J. Tokuda and N. Hata are with the National Center for Image Guided Therapy (NCIGT), Brigham and Women's Hospital, Department of Radiology, Harvard Medical School, Boston, MA, 02115 USA (e-mail: tokuda@bwh.harvard.edu, hata@bwh.harvard.edu)

X. Liu is with the New Jersey Institute of Technology, Newark, NJ 07103, USA (e-mail: xuan.liu@njit.edu)

R. Seifabadi, S. Xu and B. Wood are with the Center for Interventional Oncology, Radiology and Imaging Sciences, National Institutes of Health, Bethesda, MD, 20892, USA (e-mail: reza.seifabadi@nih.gov, xus2@cc.nih.gov, bwood@nih.gov)

G.S. Fischer is with the Automation and Interventional Medicine (AIM) Robotics Laboratory, Department of Mechanical Engineering, Worcester Polytechnic Institute, 100 Institute Road, Worcester, MA 01609, USA (e-mail: gfischer@wpi.edu)

Manuscript received 2017

\* indicates the corresponding author.

## I. INTRODUCTION

The last two decades have witnessed increased interest in MRI-guided minimally invasive interventional procedures and functional MRI (fMRI)-guided rehabilitation [1]. MRI is characterized by excellent soft tissue contrast, high spatial resolution, the use of non-ionizing radiation, and image-based tracking and guidance. Thus there is a natural clinical aspiration to use live MRI to monitor, feedback, guide, and control interventions.

During MRI-guided minimally invasive interventions, force sensing may provide important feedback that may theoretically increase the safety or accuracy of these procedures, although speculative. First, the interaction forces between the interventional tools (e.g. catheters, guide wires, needles) and the surrounding tissue provide important intraprocedural feedback to physicians. But these forces are typically indirectly measured from the proximal portion of the tools, making it less accurate and with slower response. Force sensing of the tools may be important to enable real-time monitoring and closed loop control of the procedure (i.e. controlling the ablation process with a fiber optic force sensor at the tip of the ablation catheter [2] to measure the contact forces). Second, besides direct intra-procedural monitoring, it is well-recognized that force feedback in certain minimally invasive interventions can potentially reduce errors, decrease operation times, as well as enhance psychomotor skill acquisition during training [3]. Third, since the imaging update rate of MRI is relatively low (typically less than 2-5 Hz), force sensors are ideal to provide high bandwidth interventional information. Fourth, relying purely on visual cues from imaging (without closing the loop) has been shown to saturate cognitive load [4]. Fifth, force sensing is particularly useful for robot-assisted procedures, where practitioners lose the tactile perception of the interventional procedure, which can provide additional feedback on device location within dynamic deformation of specific tissue planes.

In neuroscience and rehabilitation using functional MRI (fMRI) to study human motor control, force sensors are typically integrated with a haptic device that displays tactile sensation to the user to stimulate human's sensory-motor systems. These sensors provide repeatable experimental conditions to facilitate the investigation of the relation between human cognition and behavior. The applications range from the fMRI-compatible wrist robotic interface with fiber optic position sensor to study brain development in neonates [5] and

adults [6], to the investigation of hand precision grip control with a cable-driven fMRI-compatible haptic interface using fiber optic force sensors [7]. The sensing range and resolution of both sensors were optimized for the specific application and could readily be designed for other sensing range or resolutions (different flexure geometry or materials, detector sensitivity, etc).

With the prevalence of MRI-guided intervention and rehabilitation research and the prominence of fiber optic sensors (including force, torque and pressure sensors), fiber optic force sensing for MRI-guided procedures is a multidisciplinary area that aims to make both the interventions and rehabilitation smarter, safer and more efficient. About one decade ago, Tsekos et al. [1] reviewed sensors, actuators and robotic systems for MRI-guided interventions and rehabilitation. In 2008, Gassert et al. [8] introduced several versions of intensity based fiber optic force sensors and flexure design methodology. In 2010, Polygerinos et al. [9] reviewed fiber optic force sensors for cardiac catheterization procedures. Taffoni et al. [10] reviewed fiber optic sensors for general MRI applications. In this paper, we provide a comprehensive overview of MRI-compatible fiber optic force sensors and the state of the art development. By focusing on force sensors, we introduce different sensing principles and compare the advantages and disadvantages of each sensor for an in-depth review and intuitive introduction for developers and practitioners considering the addition of force feedback for MRI interventions and rehabilitations. These basic principles can be extended for fiber optic sensing of a plural of parameters beyond forces, including pressure, temperature, shape, vibration [11], physiological parameters [12], textile based wearable devices [13], [14], etc. Thanks to the temperature sensing capability of fiber optic sensors, they have been used for temperature monitoring during thermal treatments [15], including radiofrequency ablation, laser ablation, microwave ablation, high intensity focused ultrasound ablation, and cryoablation. This is attributed to the attractive features of fiber optic sensors, namely their flexibility, small size, accuracy, sensitivity, and immunity to MRI and adverse electromagnetic environments.

A search of the literature was conducted on six Internet databases including Google Scholar, IEEE Xplore, PubMed, ScienceDirect, Web of Science and Wiley Online Library. Two groups of keywords were used in the literature search: group 1 (“fiber optic sensor” OR “fiber optic force sensor”) and group 2 (“MRI fiber optic force sensor” OR “MRI force sensor” OR “MRI robot sensor”).

Since fiber optic sensing is inherently electric (at least at the sensor tip with appropriate material selection), fiber optic force sensors are one of the most feasible solutions to provide force sensing in the MRI environments. Fiber optic sensors for MRI environment applications consist of two subsystems: the optoelectrical subsystem and the mechanical sensing subsystem. The number of axes of a sensor is also referred as the sensing degree of freedom (DOF) for the sensor.

Fig.1 illustrates one representative system setup by Polygerinos et al. [16] that evaluated an intensity based fiber optic sensor for cardiac catheterization procedure on a healthy

swine model. Fiber optic cables passed through the MRI patch panel for communication between the sensor and signal conditioning instrumentations that include amplifier and data acquisition card. Alternatively, signal conditioning circuitry can also be placed inside the MRI room with appropriate shielding and electromechanical design of the sensor and signal conditioning circuitry as in Su et al. [17].

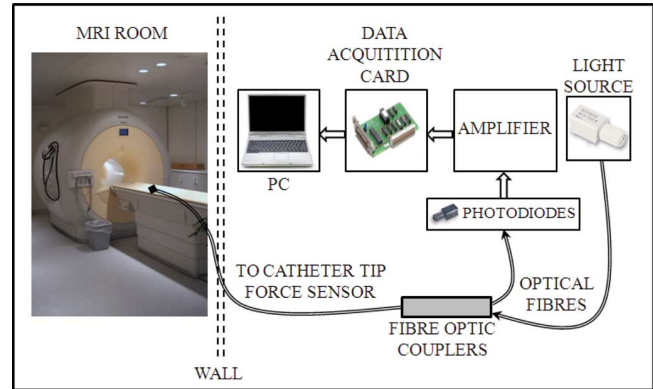


Fig. 1. One representative experimental setup for evaluation of an intensity based fiber optic sensor for cardiac catheterization procedure on a healthy swine model (Polygerinos et al. [16]). The optoelectronic equipment was placed outside the MRI room. Fiber optic cables passed through the MRI patch panel for communication between sensor and signal conditioning instrumentations ©2011 IEEE. Signal conditioning circuitry can also be placed inside the MRI room with appropriate shielding as in Su et al. [17].

#### A. MRI Safety, MRI-Compatibility Terminologies, and Compatibility Evaluation

The U.S. Food and Drug Administration (FDA) has defined the standard to quantify MRI device safety following the device classification (ASTM F2503) originally proposed by the American Society for Testing and Materials (ASTM). As shown in Table I, a device is considered “MR Safe” if it poses no known hazards in any MRI environments. “MR Conditional” is defined as an item that has been demonstrated to pose no known hazards in a specified MRI environment with specified conditions of use. These terms are about safety, while neither imaging artifacts nor device functionality is covered. Many devices are made “MRI visible” but have widely differing artifacts (blossoming and other) within a 1.5T vs a 3T strength environment.

The original “MR compatible” definition in 1997 is obsolete, but still used in the mechatronics and clinical communities. An MRI-compatible device should comply with the bidirectional MRI compatibility requirement: neither the device should disturb the scanner function and nor it should create image artifacts and the scanner should not disturb the device. The MRI system can affect the device functionality in different ways. The strong magnetic field can generate torque/force to the device, and disturb the functionality of active components. Both the pulsed gradient and RF magnetic field could induce an electrical current in the non-ferromagnetic conducting materials and electronics (like electrically active sensors).

Force sensors can potentially affect MRI imaging in two aspects. From the material perspective, flexures made of fer-

TABLE I  
ASTM F2503 CLASSIFICATION FOR THE MRI ENVIRONMENT

Symbol	Term	Definition
	MRI safe	an item that poses no known hazards in all MRI environments. "MR safe" items include non-conducting, non-metallic, non-magnetic items.
	MRI conditional	an item that has been demonstrated to pose no known hazards in a specified MRI environment with specified conditions of use. Field conditions that define the MRI environment include static magnetic field strength, spatial gradient, dB/dt (time varying magnetic fields), radio frequency (RF) fields, and specific absorption rate (SAR).
	MRI unsafe	an item that is known to pose hazards in all MRI environments.

romagnetic materials cause heavy distortion to imaging. Non-ferromagnetic conductors induce interference through magnetic field distortion and susceptibility. From the energetics perspective, electricity (i.e. the electrical current inside a strain gauge) excludes an MR-safe option, because electrical current inevitably generates electromagnetic waves causing imaging artifacts (stripes or dot type artifacts) due to the radio frequency (RF) interference. Based on the definition of "MR safe", optical sensors are essentially the only type that can be "MR safe".

To quantitatively evaluate the effects of a device on the MR image quality, two methods are typically used: 1) Signal-to-Noise Ratio analysis based on the National Electrical Manufacturers Association (NEMA) standard MS1-2008 [18] and 2) Geometric distortion analysis based on the NEMA standard (MS2-2008) [19].

### B. Design Requirements and Challenges

Besides the MRI related design constraints, fiber optic force sensors for minimally invasive interventions and rehabilitation exhibit special design challenges.

1) Sensor miniaturization: it is usually preferable to have small footprint and dimension for the fiber optic force sensor, so that it does not interfere with the instrument to which it is attached.

2) Tool integrability: even the sensor is miniaturized to an appropriate scale, sensor integration with the interventional tool to maintain its functionality may be formidably challenging. Taking laparoscopic minimally invasive surgery as an example, the sensor and tool integration problem is illustrated in [20], which shows four possible locations of sensors. Sensors could be located at the tool tips, on the tool shaft (inside or outside the patient body) or close to the actuation mechanism. The closer to the force contact spot, the higher fidelity would be, depending upon the clinical goals .

3) Sterilization and disposability : sterilization of sensorized instrument is a practical and imperative design consideration for successful clinical applications. Physical and chemical sterilization are two major approaches for tool disinfection [20]. Physical sterilization employs saturated steam to heat the equipment up to 121°C at 103k Pa above the atmospheric

pressure. Chemical sterilization uses chemical agents (i.e. hydrogen peroxide, ethylene oxide gas) and lower heat levels while it requires more time to complete the process. Even though fiber optic sensors are generally credited for better survivability in hazardous environments, meticulous design considerations are still required to ensure robustness and durability.

### C. Resistive Strain Gauge based Force Sensors in MRI Environments

Besides fiber optic sensors, resistive strain gauge [20], [21], one type of resistive sensing method, is the most popular sensing approach which has been evaluated in early MRI robotic systems. Sutherland et al. [22] reported a 3-degree-of-freedom (DOF) force/torque transducer using load cells on a titanium elastic probe. Khanicheh et al. [23] developed a variable-resistance hand device incorporating an aluminum strain gauge to investigate brain and motor performance during rehabilitation after stroke using fMRI. Vanello et al. [24] developed a glove made of a conductive elastomer with piezo-resistive properties. Tse et al. [25] designed a biopsy robot using off-the-shelf piezo-resistive sensor (FSS Sensor Technics) to perform bilateral teleoperation in MRI. Kokes et al. [26] utilized an industrial force sensor JR3 to perform teleoperated needle insertion.

The MR environment makes the use of resistive strain gauge-based sensing inside the MRI bore less viable than fiber optic sensors (essentially optical strain gauges) due to susceptibility to electrical noise and the requirement that gauges must be placed a suitable distance away from the MR field. A resistive strain gauge is one option for out of bore applications inside the MRI room and Su et al. designed a strain gauge based pneumatic haptic device [17]. Thus fiber optic sensors are better options for inside bore or close to bore applications.

## II. BASICS OF FIBER OPTIC FORCE SENSING AND FLEXURE DESIGN

In this section, we review the basics of fiber optics and the related concepts for fiber optic force sensor design. We also introduce an overview of the mechanical design of flexure mechanisms for MRI applications.

### A. Basics of Fiber Optics

Fibers are typically made of plastic or glass, with a high refractive index core and a low refractive index cladding. Light is confined in the coaxial waveguide of an optical fiber. The core of the plastic fiber typically consists of one or more acrylic-resin fibers 0.25 – 1 mm in diameter, encased in a polyethylene sheath. They constitute the majority of photoelectric sensors due to the light weight, cost effectiveness and flexibility. The glass fiber, made from silicon dioxide (also known as silica), typically consists of 10 – 100 μm diameter cores with high refractive index.

Optical fibers can be categorized as multimode or single mode, with the main difference being the core size and

propagation of light. Multimode fibers typically have a larger core compared to the cladding. Multimode fibers have large numerical aperture and therefore collect light from different angles to be coupled into fiber propagating mode. As a result, it allows high-efficient coupling of the optical signal and the use of spatially incoherent wide field light sources such as light-emitting diodes (LEDs). However, in multimode fiber, light travels in different modes and each mode corresponds to a characteristic propagation speed. This phenomenon is known as modal dispersion and poses a significant challenge in the management of light pulses and the interpretation of the measured optical signal. A single mode fiber typically has a smaller core compared to multimode fiber, depending on the operating wavelength. Due to the small diameter core of the single mode fiber, only one propagation mode of the light wave is supported in single mode fiber. Single mode fibers have an extremely low loss, preserve coherence properties of light, and therefore is one of the most widely used mediums for long distance communication.

In terms of the sensing region, there are two major categories of fiber optic sensors. Intrinsic fiber optic sensors have a sensing region within the fiber and light does not leave the fiber. In extrinsic sensors, light has to leave the fiber and reach the sensing region outside and then comes back to the fiber. According to the optical modulation mechanism, fiber optic sensors can be classified as intensity modulation, wavelength modulation, and phase modulation.

### B. Flexure Design

Flexure design is crucial for fiber optic sensors for MRI applications, as the flexure mechanism needs to meet the stiffness requirement to generate enough force sensing range while being MRI-compatible. For intrinsic sensors, the flexure is the internal structure of the fiber optic cable. For extrinsic sensors, flexure design typically uses metals, plastics or polymers. Generally, metals have better mechanical properties (higher Young's modulus and higher fatigue strength) than plastics and polymers. However, plastic and polymers exhibit better MRI compatibility.

As summarized by Gassert et al. [8], flexures for extrinsic force sensors are kinematic joints typically consisting of simple 1-DOF geometries as shown in Fig. 2 top row. Fig. 2 bottom row shows 2-DOF flexures made of 1-DOF geometries with improved compactness.

The flexure stiffness requirements [8] are determined by the force/torque range and the deflection range imposed by the optical system. The measured signal is ideally linear with respect to the flexure displacement. As demonstrated by Gassert et al. [8], the response intensity of these optical sensors as a function of the distance to the mirror (like the mirror shown in Fig. 3 (a)) can be divided into two regions: a linear region with high-sensitivity and a nonlinear region with decreasing sensitivity. As a linear response is desired, the sensor displacement should stay within the linear region of the response curve. Mechanically, the flexure determines the overall sensing bandwidth as the optical system typically has a higher bandwidth than the mechanical system. Thus the first

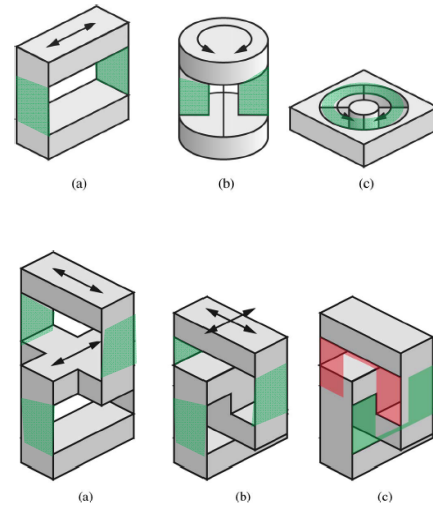


Fig. 2. Top row: typical geometries of flexure design for 1-DOF fiber optic force sensors (a) and 1-DOF fiber optic torque sensors (b-c). Bottom row: typical geometries of flexure design for 2-DOF XY fiber optic force sensor. (a) Two serially connected linear stages. (b) Shifting down the upper stage for compactness. (c) Two U-shaped linear stages. The green shades indicate the flexure joint structure. [8] ©2008 IEEE.

resonance frequency of the flexure dominates the measurement frequency [8].

### III. FIBER OPTIC FORCE SENSING PRINCIPLES

This section introduces the most common principles of fiber optic sensors and their applications in MRI-guided interventions and rehabilitation research. Table II summarizes the representative fiber optic sensors in the chronological order with key features including MRI compatibility, sensing DOF, dimension, sensing range and resolution, and applications.

#### A. Intensity Modulated Fiber Optic Force Sensor

Intensity modulated sensors rely on voltage or current measurement due to force-induced change in intensity. Thus it possesses the features of the simple design, low cost, and easy signal interpretation. Thanks to these features, intensity modulated sensors are relatively straightforward for building up multiple DOF sensors and have the most applications in robotics. Essentially, this measurement principle has two variants: reflective and transmissive sensors as shown in Fig. 3 (a) and (b) respectively. The reflective sensors rely upon light reflection [8], whereas transmissive sensors rely on light emission and single or multiple receiver sensing fiber (dual or quad elements) [27].

In 1990, Hirose and Yoneda [28] originally proposed to use a quad photo sensor to monitor the relative twist and displacement of flexure in a 6-DOF fiber optic force/torque sensor. A recent development inside MRI started from Takahashi and Tada [29], who developed a 6-DOF optical sensor using an acrylic flexible structure as the sensing element and five optical fibers as transduction element. This differential measurement method is shown in Fig. 3 (b). One emitting fiber is attached

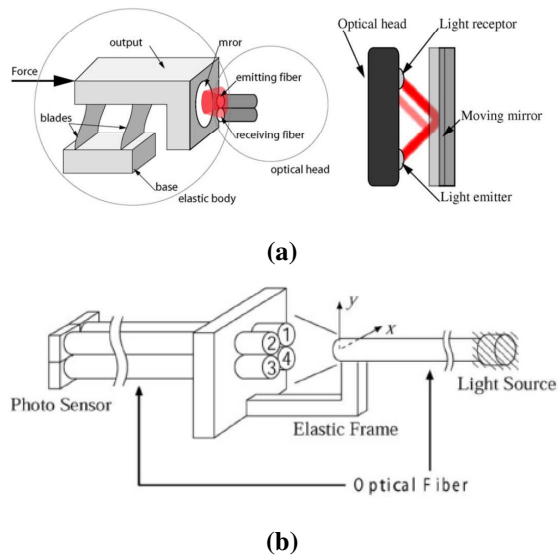


Fig. 3. Different methods to implement intensity modulation based fiber optic sensors. Reflective and transmissive are the two major styles. a) reflective fiber optic sensor [8] ©2008 IEEE; b) transmissive fiber optic sensor [27] ©2004 IEEE.

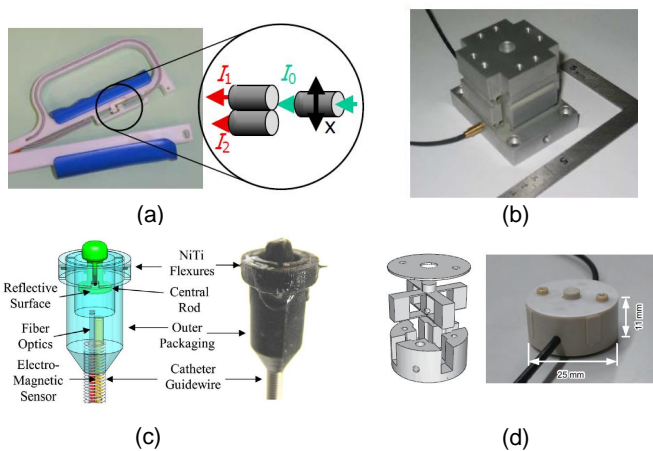


Fig. 4. Single axis intensity modulated fiber optic force sensor. a) reflective fiber optic sensor from ETH Zurich [30] to measure hand grip force during fMRI. ©2005 IEEE; b) reflective fiber optic sensor from ETH Zurich [8] to measure the grip force between the thumb and the index finger. ©2008 IEEE; c) reflective fiber optic sensor made with 3D printing from Harvard University for cardiac applications. [31] ©2010 IEEE; d) reflective fiber optic sensor with parallel plate structure from Chuo University and Advanced Industrial Science and Technology in Japan [32] ©2010 IEEE.

to the moving part and the four receiving fibers are arranged as a bundle.

Fig. 4 illustrates four examples of single axis intensity based fiber optic force sensors. In Fig. 4, (a) Riener et al. [30] proposed a similar solution to the design by Takahashi et al. [29], with differential measurement over one emitting and two receiving fibers. In Fig. 4 (b), Gassert et al. [8] designed a 2-DOF force sensor made of aluminum to aid measurement of the grip force between the thumb and the index finger during rehabilitation inside MRI. In Fig. 4 (c), Kesner et al. [31] developed an inexpensive force sensor with 3D printing technique. In Fig. 4 (d), Tokuno et al [32] developed a uni-

axial optical force sensor. The sensor head component has parallel plate structure and is made of glass fiber-reinforced polyether ether ketone (PEEK) to reduce axial interference and hysteresis characteristics of the plastic resin. However, the emission lens, encoder lens, and reception lens significantly increase the cost of this sensor.

Besides the aforementioned intensity modulated sensors that are used for image-guided interventions, intensity based fiber optic force sensor is also popular for rehabilitation and neuroscience study. Allievi and Burdet et al. [5] from Imperial College London designed and evaluated an fMRI-compatible wrist robotic interface to study brain development in neonates. Butzer and Gassert from Swiss Federal Institute of Technology (ETH Zurich) [33] designed a haptic interface for grip control study.

However, intensity modulated sensors typically suffer from intensity fluctuation either due to light source instability, fiber bending or fiber mismanagement. Another issue is that light is required to exit the fiber causing optical loss. To overcome these problems, Puangmali et al. [34] proposes to use bent tip optical fiber to reduce light loss as shown in Fig. 3 (c). Polygerinos et al. [16] as shown in Fig. 3 (d) proposed to use reference fiber to compensate for transmission losses, fiber misalignments, and fiber bending. Other methods include inclined fiber pair [35] and a single optical fiber (the same optical fiber transmits and receives the light) with an optical coupler [36].

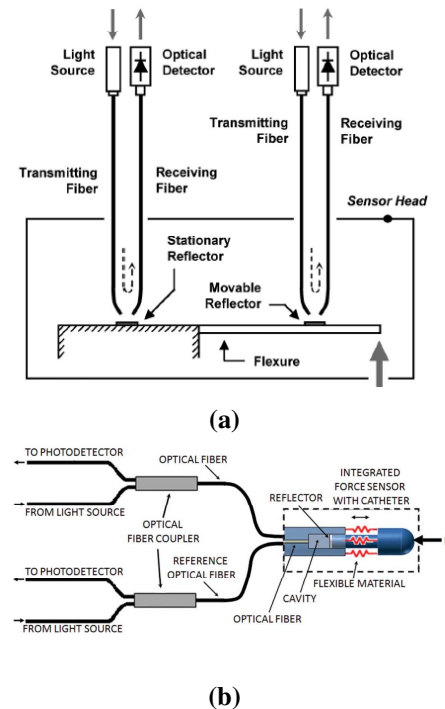


Fig. 5. Two methods to improve signal stability for intensity modulation based fiber optic sensors. a) bent tip reflective fiber optic sensor [34] ©2010 IEEE; b) reflective fiber optic sensor using coupler [37] ©2013 IEEE.

These ideas have been incorporated into the design of multiple axis sensors depicted in Fig. 6. In Fig. 6 (a), Tan et al. [35] utilized inclined fiber pair and applied Prandtl-Ishlinskii play operator to compensate hysteresis of plastic material. Since the

constituent material is Acrylonitrile Butadiene Styrene (ABS) with non-uniform mass distribution, the sensing accuracy is still limited. In Fig. 6 (b), Polygerinos et al. [37] designed a tri-axial catheter-tip force sensor for MRI-guided cardiac procedures. Its structure is similar to the one by Peirs et al. [36]. As shown in Fig. 6 (c), Su et al. [38] developed a low-cost intensity modulated force sensor with a spherical convex mirror to focus light and decrease light loss. In Fig. 6 (d), Puangmali et al. [39] proposed a bent-tip based fiber optic sensor that is compatible with laparoscopic operations and can be used to localize tissue lesions or relatively hard nodules buried under an organ's surface. Puangmali et al. proposed a mathematical model of intensity-modulated bent-tip optical fiber sensors [34], serving as a theoretical guideline for intensity modulated sensor design. The group led by Kaspar Althoefer and Hongbin Liu from the Kings College London [40] have developed a 3-DOF intensity based sensor using charge coupled device (CCD) cameras. It used image processing to read out the forces by measuring light intensity. Kalman filter technique was used to reduce the noise of the light intensity signals.

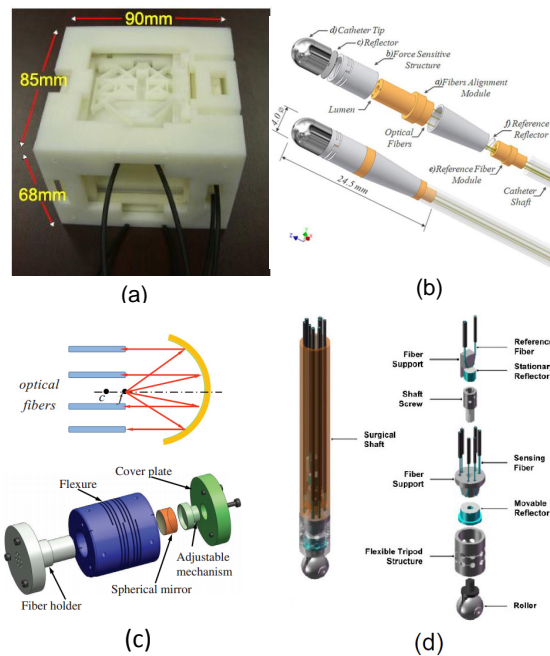


Fig. 6. Three axis intensity modulated fiber optic force sensor. a) reflective fiber optic sensor from University of Maryland for breast biopsy [41] ©2011 IEEE; b) reflective fiber optic sensor for cardiac interventions from Imperial College [16] ©2011 IEEE; c) reflective fiber optic sensor for prostate biopsy by Su et al. from Worcester Polytechnic Institute [38] ©2009 IEEE; d) reflective fiber optic sensor for minimally invasive surgical palpation from Imperial College [39] ©2012 IEEE.

### B. Wavelength Modulated Fiber Optic Force Sensor

To achieve higher sensitivity, wavelength modulated sensors provide better resolution than their intensity modulated counterparts. The fiber Bragg grating (FBG), developed in 1978 by Hill et al. [11], takes advantages of photo-sensitivity of Ge-doped fiber and a periodic change of the refractive index in the core region of an optical fiber.

If a fiber is strained from applied loads, then these gratings will change accordingly and allow a different wavelength to

be reflected back from the fiber. The reflected wavelength shift (Bragg wavelength  $\lambda_B$ ) can be expressed [55] as a function of the period of the grating  $\Lambda$  and the effective refractive index  $\eta_{eff}$  as  $\lambda_B = 2\Lambda \cdot \eta_{eff}$ . The wavelength shift change can be expressed as

$$\frac{\Delta\lambda_B}{\lambda_B} = k_\epsilon \cdot \epsilon + k_T \cdot \Delta T$$

where  $k_\epsilon$  is the coefficient for the strain  $\epsilon$  and  $k_T$  is the coefficient for the temperature change  $\Delta T$ . Calibrating the sensing equipment to read the changes in reflective index makes it possible to monitor temperature and strains by only analyzing the specific wavelength of the light source being reflected.

Endosense SA from Switzerland has developed TactiCath Quartz ablation catheter [2] (now owned by St. Jude Medical Inc., USA) as shown in Fig. 7 (a). The TactiCath catheter is an FBG based force-sensing ablation tool that provides physicians with real-time measurement of the contact force between catheter tip and tissue during the ablation procedure to treat atrial fibrillation (AF) respectively. Conventionally during the transcatheter cardiac ablation, the physician estimates the force being applied to the heart's tissue. The contact pressure acts as a surrogate and is proportional to the tissue volume that can be ablated. Thus overestimate or underestimate of contact force impacts ablation volume and could cause injury to the tissue or insufficient ablation that does not resolve AF.

A non-optical ablation catheter (THERMOCOOL SMART-TOUCH, Biosense Webster, Inc) has been developed to measure real-time catheter-tissue contact force during catheter mapping and radiofrequency ablation. It uses a small spring connecting the ablation tip electrode to the catheter shaft with a magnetic transmitter and sensors to measure the deflection of the spring. Both sensorized catheters have contact force resolution less than 1 gram in bench testing [50].

Moerman et al. [48] from the Trinity College, Ireland developed an FBG sensor that has high acquisition rate up to 100 Hz bandwidth. This design is illustrated in Fig. 7 (b). This sensor can sense force up to 15 Ne with a maximum error of 0.043 N. This computer controlled indenter aiming to provide highly repeatable tissue deformation was evaluated with indentation tests on a silicone gel phantom and the upper arm of a volunteer. Iordachita et al. [47], [56] at Johns Hopkins University have developed different versions of FBG sensor for retinal microsurgery, and Fig. 7 (c) and (d) show the 2-DOF and 3-DOF FBG sensor respectively.

Saccomandi et al. [57] developed a 1-DOF MRI-compatible force sensor for generic biomedical applications. They presented two prototypes. In one design configuration, the fiber with the FBGs was encapsulated in a polydimethylsiloxane (PDMS) sheet. In the second configuration, the fiber with the FBGs was free without the employment of any polymeric layer. Results show that the prototype which adopts the PDMS sheet had a wider range of measurement (4200 mN vs. 250 mN) and good linearity, although it has lower sensitivity.

Monfaredi et al. [49] designed an MRI-compatible 2-DOF force/torque sensor that measures  $\pm 20$ N axial force with 0.1

TABLE II

FIBER OPTIC FORCE SENSORS WITH DIFFERENT SENSING PRINCIPLES: INTENSITY MODULATION, WAVELENGTH MODULATION (FIBER BRAGG GRATING FBG) AND PHASE MODULATION (FABRY-PEROT INTERFEROMETER, FPI). NA IMPLIES THERE IS NO SPECIFICATION LISTED IN THE PAPER. AX MEANS AXIAL, RA MEANS RADIAL. <sup>a</sup>: AXIAL SENSING RANGE WAS 20N, THE RANGES OF THE OTHER 2 AXES WERE NOT AVAILABLE. <sup>b</sup>: THIS IS THE DIMENSION OF THE FLEXURE.

Author	Principle (# of fibers)	MRI compatible	DOF	Dimension: OD/L (mm)	Range	Resolution	Application
Hirose et al., 1995 [28]	Intensity (6)	No	6	76/40	980N	2.94N	General
Takahashi et al., 2003 [29]	Intensity (6)	Yes	6	NA	20N <sup>a</sup>	0.3N	Neuroscience
Peirs et al., 2004 [36]	Intensity (3)	No	3	5/11	2.5N (AX), 1.7N (RA)	0.01N	Laparoscopy
Chapuis et al., 2004 [42]	Intensity (2)	Yes	1	NA	5Nm	0.07Nm	Neuroscience
Tada et al., 2005 [43]	Intensity (4)	Yes	3	25/18	15N (AX), 8N (RA)	0.24N	General
Tokuno et al., 2008 [32]	Intensity (2)	Yes	1	25/11	3N	0.048N	General
Yokoyama et al., 2008 [2]	FBG (3)	Yes	3	3.5/NA	0.5N	10mN	Cardiac ablation
Su et al., 2009 [38]	Intensity (9)	Yes	3	25/35	10N	0.3N	Breast cancer
Iordachita et al., 2009 [44]	FBG (3)	Possible	2	0.5/NA	6.5mN	0.25mN	Ophthalmology
Yip et al., 2010 [45]	Intensity (2)	Possible	1	5.5/12	4N	0.13N	Cardiology
Su et al., 2011 [46]	FPI (1)	Yes	1	12×5×4 <sup>b</sup>	10N	1mN	Prostate cancer
Tan et al., 2011 [35]	Intensity (6)	Yes	3	49.5×48.3×50.8	7N	0.7N	Breast cancer
Kesner et al., 2011 [31]	Intensity (6)	Possible	1	6/NA	10N	0.2N	Cardiology
Polygerinos et al., 2011 [16]	Intensity (4)	Yes	1	3/18	0.85N	0.01N	Cardiology
Puangmali et al., 2012 [34]	Intensity (8)	Yes	3	10	3N (AX), 1.5N (RA)	0.02N	General
Liu et al., 2012 [47]	FPI (3)	Possible	3	0.5/NA	25mN	0.25mN	General
Moerman et al., 2012 [48]	FBG (3)	Yes	1	45/NA	15N	0.043N	General
Polygerinos et al., 2013 [37]	Intensity (4)	Yes	3	4/24.5	0.85N (AX), 0.45N (RA)	0.01N	Cardiology
Monfaredi et al., 2013 [49]	FBG (4)	Yes	2	15/20	20N (AX), 200Nmm (AX)	0.1N/1Nmm	Cardiology
Nakagawa et al., 2013 [50]	Spring deflection	No	3	3.5/NA	0.4N	10mN	Cardiac ablation
Su et al., 2013 [17]	FPI (1)	Yes	1	50×25×3.5 <sup>b</sup>	20N	1mN	Prostate cancer
Elayaperumal et al., 2014 [51]	FBG (3)	Yes	3	1.02/NA	±0.5N	0.043N	Surgical haptics
Turkseven et al., 2015 [52]	Intensity (2)	Yes	1	NA	7N	NA	Rehabilitation
Butzer et al., 2015 [33]	Intensity (2)	Yes	1	10×29.7×60	3N	0.01N	Neuroscience
Qiu et al., 2016 [53]	FPI (1)	Possible	1	1.88/NA	1.2N	0.25mN	Tissue mechanics
Noh et al., 2016 [40]	Intensity (2)	Yes	3	3.5/13	1N (AX), 0.5N (RA)	0.25mN	Cardiology
Xu et al., 2016 [54]	FBG (3)	Yes	2	2/NA	NA(AX), 1.57N (RA)	0.01N	Continuum robot

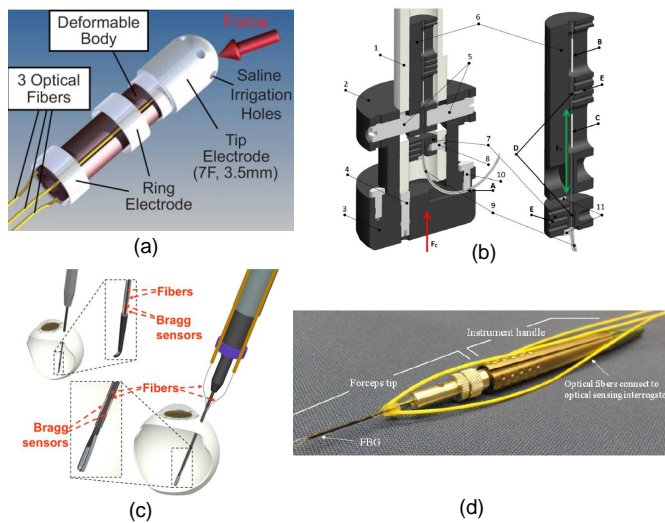


Fig. 7. FBG fiber optic force sensors. a) FBG sensor TactiCath developed by Endosense SA in collaboration with Stanford University for atrial fibrillation [2] ©2008 American Heart Association; b) A soft tissue indenter with 1-DOF FBG force sensing developed at Trinity College, Ireland [48] ©2012 Elsevier B.V.; c) 2-DOF FBG sensor for retinal microsurgery developed at Johns Hopkins University [44] ©2009 Springer; d) 3-DOF FBG sensor for retinal microsurgery developed at Johns Hopkins University [47], [56] ©2012 SPIE.

N resolution, and ±200 Nmm axial torque with 1 Nmm resolution. This compact sensor (15 mm diameter, 20 mm height) includes active element (bronze and brass) manufactured by wire Electrical Discharge Machining (EDM) and then were

bonded with high strength plastic steel epoxy. The casings were made of 3D printed ABS material.

The haptics group at the Stanford University led by Mark Cutkosky has developed several iterations of FBG sensor for needle shape sensing [55] and force sensing [51]. Elayaperumal et al. [51] designed a 3-DOF FBG force sensor to measure the insertion force at the needle tip. They evaluated the benefit of haptic feedback with an agar phantom with membranes made of Shore 2A durometer silicone that mimics the connective tissue layer in natural visceral membranes. It was demonstrated that the success rate of the identifying membrane was 75.0% with FG force feedback and 33.3% in the case without haptic feedback.

A distinct feature of FBG sensors is its ability to perform optical multiplexing, namely, the capability to measure strain from multiple FBGs along a single fiber. Thus it is popular for shape sensing of a curved instrument, and this has been used for concentric tube robot shape sensing [58] and surgical needles [59]. Xu et al. [54] led by Rajni Patel at the University of Western Ontario designed a helically wrapped FBG sensor. Three FBG sensors were embedded into a pre-curved Nitinol tube (one type of continuum robots) to measure curvature, torsion, and force sensing in continuum robots.

FBG sensors are attractive as they use fiber with small diameter (e.g. 126 μm) and can be embedded into mm scale instruments. Moreover, its multiplexing capability enables multiple parameter sensing at different locations as demonstrated in [54]. FBG sensors are sensitive to temperature, thus

it requires temperature compensation. One key drawback of FBG force sensors is the system cost and complicated system setup. FBG typically requires both a costly optical source and a spectral analysis equipment.

### C. Phase Modulated Fiber Optic Force Sensors

Phase modulated fiber optic force sensing is based on interferometry [60] that provides displacement sensing (thus force sensing) through the measurement of a relative phase shift between light beams. Light interferometers include two beam configurations such as Michelson and Mach-Zehnder interferometers and multiple beam configurations such as Fabry-Perot interferometers.

Inside a Fabry-Perot strain sensor, light propagates between a pair of partially reflective mirrors that form a Fabry-Perot cavity. A portion of light exits and the rest remains inside the cavity. Multiple beams with different optical path lengths exiting the Fabry-Perot cavity are superimposed, generating destructive and constructive interference that can be observed in the spatial domain or spectral domain. The phase of interference signal varies as the change in Fabry-Perot cavity length denoted as  $\delta$ . As shown in Fig. 8,  $L_{cavity}$  is the original cavity length. For Fabry-Perot force sensors,  $\delta$  is proportional to the gauge length (the active sensing region, defined as the distance between the end mirrors of the Fabry-Perot cavity), and proportional to the force exerted. The returning light interferes resulting in black and white bands known as fringes caused by destructive and constructive interference. The intensity of these fringes varies due to a change in the optical path length related to a change in cavity length when uni-axial force is applied. The sensing principle is shown in Fig. 8 [46].

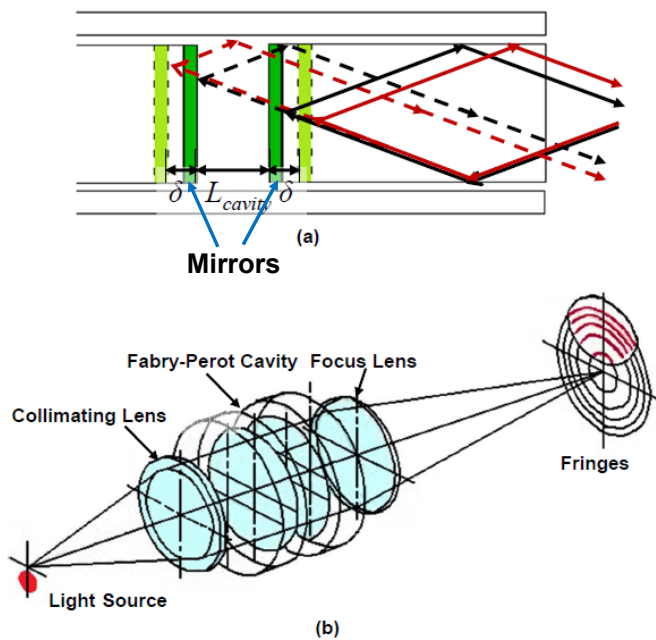


Fig. 8. The Fabry-Perot sensing principle and its light propagation in Fabry-Perot cavity (a) and one type of implementation (b) [46] ©IEEE 2011.

This phenomenon can be quantified through the summation of two waves [11]. By multiplying the complex conjugate and

applying Euler's identity, we obtain the following equation of reflected intensity at a given power for planar wave fronts:

$$I = A_1^2 + A_2^2 + 2A_1A_2\cos(\phi_1 - \phi_2) \quad (1)$$

with  $A_1$  and  $A_2$  representing the amplitude coefficients of the reflected signals.  $\phi_1$  and  $\phi_2$  are the light phases. The above equation can be changed to represent only intensities by substituting  $A_i^2 = I_i (i = 1, 2)$  and  $\phi_1 - \phi_2 = \Delta\phi$  as

$$I = I_1 + I_2 + 2\sqrt{I_1I_2}\cos\Delta\phi \quad (2)$$

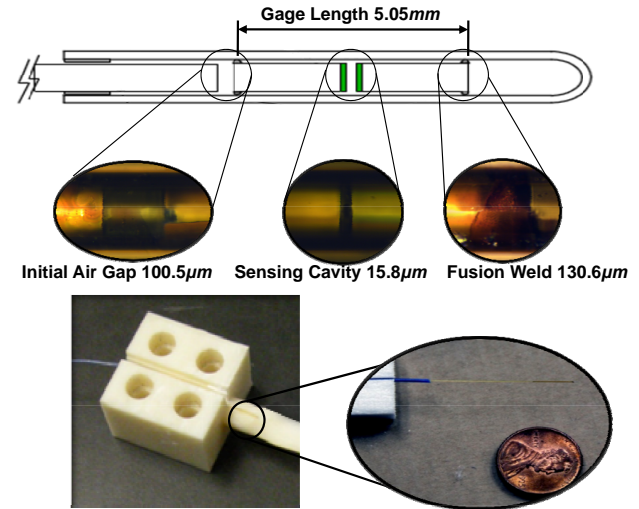


Fig. 9. (Top) magnified FPI strain sensor with three segment dimension, (bottom) example FPI configuration embedded in an ABS cantilever beam and the inset shows the fiber with a cent [46] ©IEEE 2011.

Su et al. [17], [46] designed an FPI fiber optic strain sensor utilizing a commercially available FPI strain gauge (FOS-N-BA-C1-F1-M2-R1-ST, FISO Technologies, Canada) for MRI-guided needle placement. As shown in Fig. 9, the main component of the FPI is the sensing cavity, measuring  $15.8\mu m$  wide. A glass capillary covering the sensing region is fusion welded to the fiber in two locations and encapsulates the sensor. There is an air gap of approximately  $100.5\mu m$  wide. The total length of the FPI sensor, including the glass capillary, and bare fiber is approximately  $20mm$ .

Qiu et al. [53] designed and developed an FPI fiber optic force sensor that enables in situ quantification of tissue elasticity. The device (Fig. 10 (a)) allowed intraoperative characterization of stiffness for tissue classification and surgical guidance [61]–[63]. The optical signal from the force sensing device was interrogated by a spectral domain OCT engine at  $1.3\mu m$ . Signal processing was implemented in real-time using graphic processing unit (GPU). As shown in Fig. 10 (b), the FP cavity for force sensing was integrated into the distal tip of the probe. The miniature probe (qOCE probe) was used to induce sample deformation through uniaxial compression and the force exerted was quantified by measuring the phase shift in optical signal due to probe shaft deformation (Fig. 10 (c)). In addition, the optical signal from the sample under compression was also acquired and analyzed for sample deformation tracking (Fig. 10 (d)). Through simultaneous quantification

of force/stress and sample deformation/strain, tissue elasticity could be quantified using the stress-strain curve obtained (Fig. 10 (e)).

The advantages of FPI sensors include high sensitivity and robust to a large range of temperature variation ( $-40^{\circ}\sim 250^{\circ}$ ) due to air gap insulation to the sensing region. FPI sensor by Su et al. [17] is voltage measurement based and is relatively low cost. But premium FPI sensors (i.e. [53]) could be very costly due to the use of light source and detector. Individual FPI instrument for force sensing needs calibration and may require repeated calibration over time.

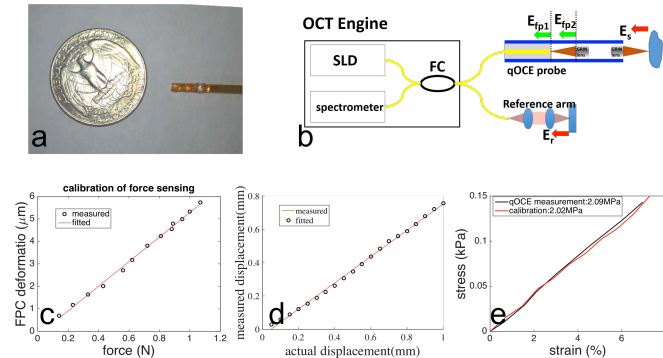


Fig. 10. Prototype and calibration of the quantitative optical coherence elastography (qOCE) probe developed at the New Jersey Institute of Technology. (a) Photo of qOCE probe in comparison with a US quarter. (b) The optical system of the qOCE system. (c) Results of force calibration show FP cavity deforms proportionally to force exerted. (d) Calibration results show displacement obtained from Doppler OCT signal is linearly related to actual displacement. (e) Stress-strain curve obtained using qOCE measurement (black) and calibration of strain-stress curve (red). [53] ©OSA publishing 2016

#### IV. DISCUSSION AND FUTURE PERSPECTIVES

This paper reviews the classification and principles of fiber optic force sensors, the state of the art in optical sensing, advantages and disadvantages of each sensor, and their possible clinical applications. Intensity modulation based force sensing provides a simple and low-cost solution using voltage or current measurement. Thus as shown in Table II, a majority of fiber optic force sensors are intensity modulated. But typically their sensitivity is relatively low. Fiber Bragg grating sensors [54] provide a viable solution in terms of sensing accuracy, multiplexing capability, and small fiber diameters. FBG sensors are attractive as they use fibers with small diameters (e.g.  $125\ \mu\text{m}$ ) and can be embedded into mm scale instruments. However, the costly optical source, FBG fibers and spectral analysis equipment present challenges for vast adoption of this technology. FPI fiber optic sensor provides an amiable solution for high-resolution force sensing that only relies on simple interference pattern based voltage measurement [17]. Premium FPI sensors (i.e. [53]) could be costly due to the use of special light source and detector.

Relying on fiber optic force sensors, future surgical interventions or rehabilitation will be able to provide situational awareness to augment or complement human perception in these procedures. Recently Wang et al. [64] proposed an approach for using force-controlled exploration data to update

and register an a-priori virtual fixture geometry to a corresponding deformed and displaced physical environment. Thus future procedure will be safer and more intuitive thanks to the force sensors.

Future surgical interventions or rehabilitation will rely on intelligent force sensors to provide situational awareness to augment or complement human perception in these procedures.

MRI-compatible fiber optic sensors can also be used in non-MRI environments with the similar favorable advantages. The light intensity based fiber optic sensors could be designed with low cost and relatively high sensitivity. This has potential applications in robotics research and industry, including force control in assistive robots and optic load cells for assembly and manufacturing, etc. Recently, optical sensing is being used for soft robots as optics does not rely on rigid medium, thus is "soft" in nature. Park et al. [65] developed highly stretchable optical sensors for pressure, strain, and curvature measurement. The next generation of this sensor aimed to use optical fibers to transmit and detect light through the soft waveguide instead of directly embedding a light source and a detector in the soft material. Optical fibers will allow further minimization of the size of the sensor but also to simplify the manufacturing process by removing multiple rigid components, such as LEDs, and photodiodes. Zhao et al. [66] designed stretchable waveguides to sense strain, bending and pressure of a soft prosthetic hand to distinguish the surface texture and stiffness of objects.

Beyond the fiber optic sensors for MRI environments, more techniques for fiber optic sensing are emerging. Yan et al. [67] demonstrated the feasibility of in vivo cancer detection in real time during prostate biopsy by observing the force patterns for tumor and normal tissue. Using a mechanical model, Beekmans et al. [68] developed an FPI based fiber optic sensor to measure the Young's Modulus of the bovine liver tissue embedded in gelatin and demonstrated its feasibility. Philips Research in Netherlands [69] developed an optical imaging using Diffuse Reflectance Spectroscopy (DRS) that can distinguish different tissue types through a specific "optical fingerprint". It is expected that those emerging techniques could further improve the efficacy of fiber optic force sensors in image-guided interventions and rehabilitation research.

Fiber optic sensors have begun to demonstrate their functionality and feasibility for certain interventions and rehabilitation, but it is expected that more systematic studies can potentially validate and expand their clinical value.

#### V. ACKNOWLEDGMENTS

This work is supported in part by the Congressionally Directed Medical Research Programs Prostate Cancer Research Program New Investigator Award W81XWH-09-1-0191, the Intramural Research Program of the NIH, NIH R01CA166379, NIH R01CA111288, and Link Foundation Fellowships in Advanced Simulation and Training.

#### REFERENCES

[1] N. Tsekos, A. Khanicheh, E. Christoforou, and C. Mavroidis, "Magnetic resonance-compatible robotic and mechatronics systems for image-

- guided interventions and rehabilitation: a review study,” *Annu. Rev. Biomed. Eng.*, vol. 9, pp. 351–387, 2007.
- [2] K. Yokoyama, H. Nakagawa, D. C. Shah, H. Lambert, G. Leo, N. Aeby, A. Ikeda, J. V. Pitha, T. Sharma, R. Lazzara, *et al.*, “Novel contact force sensor incorporated in irrigated radiofrequency ablation catheter predicts lesion size and incidence of steam pop and thrombus,” *Circulation: Arrhythmia and Electrophysiology*, vol. 1, no. 5, pp. 354–362, 2008.
  - [3] O. Van der Meijden and M. Schijven, “The value of haptic feedback in conventional and robot-assisted minimal invasive surgery and virtual reality training: a current review,” *Surgical Endoscopy*, vol. 23, no. 6, pp. 1180–1190, 2009.
  - [4] C. G. Cao, M. Zhou, D. B. Jones, and S. D. Schwartzberg, “Can surgeons think and operate with haptics at the same time?,” *Journal of Gastrointestinal Surgery*, vol. 11, no. 11, pp. 1564–1569, 2007.
  - [5] A. Allievi, A. Melendez-Calderon, T. Arichi, A. Edwards, and E. Burdet, “An fMRI compatible wrist robotic interface to study brain development in neonates,” *Annals of Biomedical Engineering*, vol. 41, no. 6, pp. 1181–1192, 2013.
  - [6] F. Sergi, A. C. Erwin, and M. K. O’Malley, “Interaction control capabilities of an MR-compatible compliant actuator for wrist sensorimotor protocols during fMRI,” *IEEE/ASME Transactions on Mechatronics*, vol. 20, no. 6, pp. 2678–2690, 2015.
  - [7] B. Vigar, J. Sulzer, and R. Gassert, “Design and evaluation of a cable-driven fMRI-compatible haptic interface to investigate precision grip control,” *IEEE Transactions on Haptics*, vol. 9, no. 1, pp. 20–32, 2016.
  - [8] R. Gassert, D. Chapuis, H. Bleuler, and E. Burdet, “Sensors for applications in magnetic resonance environments,” *IEEE/ASME Transactions on Mechatronics*, vol. 13, no. 3, pp. 335–344, 2008.
  - [9] P. Polygerinos, D. Zbyszewski, T. Schaeffter, R. Razavi, L. Seneviratne, and K. Althoefer, “MRI-compatible fiber-optic force sensors for catheterization procedures,” *Sensors Journal, IEEE*, vol. 10, pp. 1598–1608, Oct. 2010.
  - [10] F. Taffoni, D. Formica, P. Saccomandi, G. D. Pino, and E. Schena, “Optical fiber-based MR-compatible sensors for medical applications: An overview,” *Sensors*, vol. 13, no. 10, pp. 14105–14120, 2013.
  - [11] T. K. Gangopadhyay, “Prospects for fiber Bragg gratings and Fabry-Perot interferometers in fiber optic vibration sensing,” *Sensors and Actuators A: Physical*, vol. 113, no. 1, pp. 20–38, 2004.
  - [12] Ł. ukasz Dziuda, “Fiber-optic sensors for monitoring patient physiological parameters: a review of applicable technologies and relevance to use during magnetic resonance imaging procedures,” *Journal of biomedical optics*, vol. 20, no. 1, pp. 010901–010901, 2015.
  - [13] J. Witt, F. Narbonneau, M. Schukar, K. Krebber, J. De Jonckheere, M. Jeanne, D. Kinet, B. Paquet, A. Depre, L. T. D’Angelo, *et al.*, “Medical textiles with embedded fiber optic sensors for monitoring of respiratory movement,” *IEEE Sensors Journal*, vol. 12, no. 1, pp. 246–254, 2012.
  - [14] C. Massaroni, P. Saccomandi, and E. Schena, “Medical smart textiles based on fiber optic technology: an overview,” *Journal of Functional Biomaterials*, vol. 6, no. 2, pp. 204–221, 2015.
  - [15] E. Schena, D. Tosi, P. Saccomandi, E. Lewis, and T. Kim, “Fiber optic sensors for temperature monitoring during thermal treatments: an overview,” *Sensors*, vol. 16, no. 7, pp. 1144, 2016.
  - [16] P. Polygerinos, A. Ataollahi, T. Schaeffter, R. Razavi, L. D. Seneviratne, and K. Althoefer, “MRI-compatible intensity-modulated force sensor for cardiac catheterization procedures,” *IEEE Trans. Biomed. Engineering*, vol. 58, no. 3, pp. 721–726, 2011.
  - [17] W. Shang, H. Su, G. Li, and G. S. Fischer, “Teleoperation system with hybrid pneumatic-piezoelectric actuation for MRI-guided needle insertion with haptic feedback,” in *2013 IEEE/RSJ International Conference on Intelligent Robots and Systems (IROS)*, pp. 4092–4098, Nov 2013.
  - [18] *Determination of Signal-to-Noise Ratio (SNR) in Diagnostic Magnetic Resonance Imaging, NEMA Standard Publication MS 1-2008*. The Association of Electrical and Medical Imaging Equipment Manufacturers, 2008.
  - [19] *Determination of Image Uniformity in Diagnostic Magnetic Resonance Images, NEMA Standards Publication MS 3-2008*. The Association of Electrical and Medical Imaging Equipment Manufacturers, 2008.
  - [20] P. Puangmali, K. Althoefer, L. Seneviratne, D. Murphy, and P. Dasgupta, “State-of-the-art in force and tactile sensing for minimally invasive surgery,” *Sensors Journal, IEEE*, vol. 8, pp. 371–381, April 2008.
  - [21] Z. Lu, P. Chen, and W. Lin, “Force sensing and control in micromanipulation,” *Systems, Man, and Cybernetics, Part C: Applications and Reviews, IEEE Transactions on*, vol. 36, pp. 713–724, nov. 2006.
  - [22] G. R. Sutherland, I. Latour, A. D. Greer, T. Fielding, G. Feil, and P. Newhook, “An image-guided magnetic resonance-compatible surgical robot,” *Neurosurgery*, vol. 62, pp. 286–92; discussion 292–3, Feb 2008.
  - [23] A. Khanicheh, A. Muto, C. Triantafyllou, B. Weinberg, L. Astrakas, A. Tzika, and C. Mavroidis, “MR compatible ERF driven hand rehabilitation device,” in *Rehabilitation Robotics, 2005. ICORR 2005. 9th International Conference on*, pp. 7–12, june-july 2005.
  - [24] N. Vanello, V. Hartwig, M. Tesconi, E. Ricciardi, A. Tognetti, G. Zupone, R. Gassert, D. Chapuis, N. Sgambelluri, E. Scilingo, G. Giovannetti, V. Positano, M. Santarelli, A. Bicchi, P. Pietrini, D. D. Rossi, and L. Landini, “Sensing glove for brain studies: design and assessment of its compatibility for fMRI with a robust test,” *IEEE/ASME Transactions on Mechatronics*, vol. 13, no. 3, pp. 345–354, 2008.
  - [25] Z. Tse, E. Elhawary, M. Rea, I. Young, B. Davis, and M. Lamperth, “A haptic unit designed for magnetic-resonance-guided biopsy,” *Proceedings of the Institution of Mechanical Engineers, Part H (Journal of Engineering in Medicine)*, vol. 223, no. H2, pp. 159–72, 2009.
  - [26] R. Kokes, K. Lister, R. Gullapalli, B. Zhang, A. MacMillan, H. Richard, and J. P. Desai, “Towards a teleoperated needle driver robot with haptic feedback for RFA of breast tumors under continuous MRI,” *Medical Image Analysis*, vol. 13, no. 3, pp. 445–455, 2009.
  - [27] M. Tada and T. Kanade, “Development of an MR-compatible optical force sensor,” vol. Vol.3 of *Conference Proceedings. 26th Annual International Conference of the IEEE Engineering in Medicine and Biology Society*, (Piscataway, NJ, USA), pp. 2022–5, IEEE, 2004.
  - [28] S. Hirose and K. Yoneda, “Development of optical six-axial force sensor and its signal calibration considering nonlinear interference,” in *Robotics and Automation, 1990. Proceedings., 1990 IEEE International Conference on*, pp. 46–53 vol.1, may 1990.
  - [29] N. Takahashi, M. Tada, J. Ueda, Y. Matsumoto, and T. Ogasawara, “An optical 6-axis force sensor for brain function analysis using fMRI,” in *Sensors, 2003. Proceedings of IEEE*, vol. 1, pp. 253–258 Vol.1, Oct. 2003.
  - [30] R. Riener, T. Villgratner, R. Kleiser, T. Nef, and S. Kollias, “fMRI-Compatible Electromagnetic Haptic Interface,” in *Engineering in Medicine and Biology Society, 2005. IEEE-EMBS 2005. 27th Annual International Conference of the*, pp. 7024–7027, Jan. 2005.
  - [31] S. Kesner and R. Howe, “Design principles for rapid prototyping forces sensors using 3-D printing,” *Mechatronics, IEEE/ASME Transactions on*, vol. 16, pp. 866–870, Oct. 2011.
  - [32] T. Tokuno, M. Tada, and K. Umeda, “High-precision MRI-compatible force sensor with parallel plate structure,” *Proceedings of the 2nd Biennial IEEE/RAS-EMBS International Conference on Biomedical Robotics and Biomechanics, BioRob 2008*, (Scottsdale, AZ, United States), pp. 33–38, Inst. of Elec. and Elec. Eng. Computer Society, 2008.
  - [33] T. Bützer, B. Vigar, and R. Gassert, “Design and evaluation of a compact, integrated fMRI-compatible force sensor printed by additive manufacturing,” in *World Haptics Conference (WHC), 2015 IEEE*, pp. 158–164, IEEE, 2015.
  - [34] P. Puangmali, K. Althoefer, and L. Seneviratne, “Mathematical modeling of intensity-modulated bent-tip optical fiber displacement sensors,” *Instrumentation and Measurement, IEEE Transactions on*, vol. 59, pp. 283–291, Feb. 2010.
  - [35] U.-X. Tan, B. Yang, R. P. Gullapalli, and J. P. Desai, “Triaxial MRI-compatible fiber-optic force sensor,” *IEEE Transactions on Robotics*, vol. 27, no. 1, pp. 65–74, 2011.
  - [36] J. Peirs, J. Clijnen, D. Reynaerts, H. V. Brussel, P. Herijgers, B. Corteville, and S. Boone, “A micro optical force sensor for force feedback during minimally invasive robotic surgery,” *Sensors and Actuators A: Physical*, vol. 115, no. 2C3, pp. 447–455, 2004.
  - [37] P. Polygerinos, L. Seneviratne, R. Razavi, T. Schaeffter, and K. Althoefer, “Triaxial catheter-tip force sensor for MRI-guided cardiac procedures,” *Mechatronics, IEEE/ASME Transactions on*, vol. 18, pp. 386–396, feb. 2013.
  - [38] H. Su and G. Fischer, “A 3-axis optical force/torque sensor for prostate needle placement in magnetic resonance imaging environments,” *2nd Annual IEEE International Conference on Technologies for Practical Robot Applications*, (Boston, MA, USA), pp. 5–9, IEEE, 2009.
  - [39] P. Puangmali, H. Liu, L. Seneviratne, P. Dasgupta, and K. Althoefer, “Miniature 3-axis distal force sensor for minimally invasive surgical palpation,” *Mechatronics, IEEE/ASME Transactions on*, vol. 17, pp. 646–656, aug. 2012.
  - [40] Y. Noh, H. Liu, S. Sareh, D. S. C. K. Vithanage, H. Wurdemann, K. Rhode, and K. Althoefer, “Image-based optical miniaturized three-axis force sensor for cardiac catheterization,” *IEEE Sensors Journal*, vol. PP, no. 99, pp. 1–9, 2016.
  - [41] B. Yang, U.-X. Tan, A. B. McMillan, R. Gullapalli, and J. P. Desai, “Design and control of a 1-DOF MRI-compatible pneumatically actuated robot with long transmission lines,” *Mechatronics, IEEE/ASME Transactions on*, vol. 16, no. 6, pp. 1040–1048, 2011.

- [42] D. Chaptuis, R. Gassert, L. Sacher, E. Burdet, and H. Bleuler, "Design of a simple MRI/fMRI compatible force/torque sensor," in *Intelligent Robots and Systems, 2004. (IROS 2004). Proceedings. 2004 IEEE/RSJ International Conference on*, vol. 3, pp. 2593–2599 vol.3, sept.-2 oct. 2004.
- [43] M. Tada and T. Kanade, "Design of an MR-compatible three-axis force sensor," in *Intelligent Robots and Systems, 2005. (IROS 2005). 2005 IEEE/RSJ International Conference on*, pp. 3505–3510, Aug. 2005.
- [44] I. Iordachita, Z. Sun, M. Balicki, J. U. Kang, S. J. Phee, J. Handa, P. Gehlbach, and R. Taylor, "A sub-millimetric, 0.25 mm resolution fully integrated fiber-optic force-sensing tool for retinal microsurgery," *International Journal of Computer Assisted Radiology and Surgery*, vol. 4, no. 4, pp. 383–390, 2009.
- [45] M. C. Yip, S. G. Yuen, and R. D. Howe, "A robust uniaxial force sensor for minimally invasive surgery," *IEEE transactions on biomedical engineering*, vol. 57, no. 5, pp. 1008–1011, 2010.
- [46] H. Su, M. Zervas, G. A. Cole, C. Furlong, and G. S. Fischer, "Real-time MRI-guided needle placement robot with integrated fiber optic force sensing," in *Robotics and Automation (ICRA), 2011 IEEE International Conference on*, pp. 1583–1588, IEEE, 2011.
- [47] X. Liu, I. I. Iordachita, X. He, R. H. Taylor, and J. U. Kang, "Miniature fiber-optic force sensor based on low-coherence fabry-perot interferometry for vitreoretinal microsurgery," *Biomedical optics express*, vol. 3, no. 5, pp. 1062–1076, 2012.
- [48] K. M. Moerman, A. M. Sprengers, A. J. Nederveen, and C. K. Simms, "A novel MRI compatible soft tissue indenter and fibre bragg grating force sensor," *Medical Engineering & Physics*, pp. 1350–4533, 2012.
- [49] R. Monfaredi, R. Seifabadi, G. Fichtinger, and I. Iordachita, "Design of a decoupled MRI-compatible force sensor using fiber Bragg grating sensors for robot-assisted prostate interventions," in *SPIE Medical Imaging*, pp. 867118–867118, International Society for Optics and Photonics, 2013.
- [50] H. Nakagawa, J. Kautzner, A. Natale, P. Peichl, R. Cihak, D. Wichterle, A. Ikeda, P. Santangeli, L. Di Biase, and W. M. Jackman, "Locations of high contact force during left atrial mapping in atrial fibrillation patients: electrogram amplitude and impedance are poor predictors of electrode-tissue contact force for ablation of atrial fibrillation," *Circulation: Arrhythmia and Electrophysiology*, vol. 6, no. 4, pp. 746–753, 2013.
- [51] S. Elayaperumal, J. H. Bae, B. L. Daniel, and M. R. Cutkosky, "Detection of membrane puncture with haptic feedback using a tip-force sensing needle," in *2014 IEEE/RSJ International Conference on Intelligent Robots and Systems*, pp. 3975–3981, IEEE, 2014.
- [52] M. Turkseven and J. Ueda, "Analysis of an MRI compatible force sensor for sensitivity and precision," *IEEE Sensors Journal*, vol. 13, no. 2, pp. 476–486, 2013.
- [53] Y. Qiu, Y. Wang, Y. Xu, N. Chandra, J. Haorah, B. Hubbi, B. J. Pfister, and X. Liu, "Quantitative optical coherence elastography based on fiber-optic probe for in situ measurement of tissue mechanical properties," *Biomedical optics express*, vol. 7, no. 2, pp. 688–700, 2016.
- [54] R. Xu, A. Yurkewich, and R. V. Patel, "Curvature, torsion, and force sensing in continuum robots using helically wrapped FBG sensors," *IEEE Robotics and Automation Letters*, vol. 1, no. 2, pp. 1052–1059, 2016.
- [55] Y.-L. Park, S. Elayaperumal, B. Daniel, S. C. Ryu, M. Shin, J. Savall, R. Black, B. Moslehi, and M. Cutkosky, "Real-time estimation of 3-D needle shape and deflection for MRI-guided interventions," *Mechatronics, IEEE/ASME Transactions on*, vol. 15, pp. 906–915, Dec. 2010.
- [56] X. He, M. A. Balicki, J. U. Kang, P. L. Gehlbach, J. T. Handa, R. H. Taylor, and I. I. Iordachita, "Force sensing micro-forceps with integrated fiber Bragg grating for vitreoretinal surgery," in *SPIE BIOS*, pp. 82180W–82180W, International Society for Optics and Photonics, 2012.
- [57] P. Saccomandi, M. Caponero, A. Polimadei, M. Francomano, D. Formica, D. Accoto, E. Tamilia, F. Taffoni, G. Di Pino, and E. Schena, "An MR-compatible force sensor based on FBG technology for biomedical application," in *Engineering in Medicine and Biology Society (EMBC), 2014 36th Annual International Conference of the IEEE*, pp. 5731–5734, Aug 2014.
- [58] S. C. Ryu and P. E. Dupont, "FBG-based shape sensing tubes for continuum robots," in *2014 IEEE International Conference on Robotics and Automation (ICRA)*, pp. 3531–3537, IEEE, 2014.
- [59] R. J. Roesthuis, M. Kemp, J. J. van den Dobbela, and S. Misra, "Three-dimensional needle shape reconstruction using an array of fiber Bragg grating sensors," *IEEE/ASME transactions on mechatronics*, vol. 19, no. 4, pp. 1115–1126, 2014.
- [60] S. Yin, P. B. Ruffin, and F. T. Yu, *Fiber Optic Sensors*. CRC Press, 2008.
- [61] B. F. Kennedy, X. Liang, S. G. Adie, D. K. Gerstmann, B. C. Quirk, S. A. Boppart, and D. D. Sampson, "In vivo three-dimensional optical coherence elastography," *Optics Express*, vol. 19, no. 7, pp. 6623–6634, 2011.
- [62] T.-M. Nguyen, S. Song, B. Arnal, Z. Huang, M. O'Donnell, and R. K. Wang, "Visualizing ultrasonically induced shear wave propagation using phase-sensitive optical coherence tomography for dynamic elastography," *Optics letters*, vol. 39, no. 4, pp. 838–841, 2014.
- [63] X. Liang and S. Boppart, "Biomechanical properties of in vivo human skin from dynamic optical coherence elastography," *Biomedical Engineering, IEEE Transactions on*, vol. 57, no. 4, pp. 953–959, 2010.
- [64] L. Wang, Z. Chen, P. Chalasani, J. Pile, P. Kazanzides, R. H. Taylor, and N. Simaan, "Updating virtual fixtures from exploration data in force-controlled model-based telemanipulation," in *ASME 2016 International Design Engineering Technical Conferences and Computers and Information in Engineering Conference*, pp. V05AT07A031–V05AT07A031, American Society of Mechanical Engineers, 2016.
- [65] C. To, T. L. Hellebrekers, and Y.-L. Park, "Highly stretchable optical sensors for pressure, strain, and curvature measurement," in *Intelligent Robots and Systems (IROS), 2015 IEEE/RSJ International Conference on*, pp. 5898–5903, IEEE, 2015.
- [66] H. Zhao, K. O'Brien, S. Li, and R. F. Shepherd, "Optoelectronically innervated soft prosthetic hand via stretchable optical waveguides," *Science Robotics*, vol. 1, no. 1, p. eaai7529, 2016.
- [67] K. Yan, T. Podder, L. Li, J. Joseph, D. Rubens, E. Messing, L. Liao, and Y. Yu, "A real-time prostate cancer detection technique using needle insertion force and patient-specific criteria during percutaneous intervention," *Medical physics*, vol. 36, no. 9, pp. 4184–4190, 2009.
- [68] S. Beekmans and D. Iannuzzi, "Characterizing tissue stiffness at the tip of a rigid needle using an opto-mechanical force sensor," *Biomedical microdevices*, vol. 18, no. 1, pp. 1–8, 2016.
- [69] D. Evers, R. Nachabe, D. Hompes, F. van Coevorden, G. Lucassen, B. Hendriks, M.-L. van Velthuysen, J. Wesseling, and T. Ruers, "Optical sensing for tumor detection in the liver," *European Journal of Surgical Oncology (EJSO)*, vol. 39, no. 1, pp. 68–75, 2013.